# Colossal Permittivity in Ultrafine Grain Size BaTiO3–x and Ba0.95La0.05TiO3–x Materials

Sophie Guillemet, Zarel Valdez Nava, Christophe Tenailleau, Thierry Lebey, Bernard Durand, Jean-Yves Chane-Ching

DOI: 10.1002/adma.200700245

# Colossal Permittivity in Ultrafine Grain Size $BaTiO_{3-x}$ and $Ba_{0.95}La_{0.05}TiO_{3-x}$ Materials**

By *Sophie Guillemet-Fritsch*, *Zarel Valdez-Nava*, *Christophe Tenailleau*, *Thierry Lebey*, *Bernard Durand*, and *Jean-Yves Chane-Ching**

Development of microelectronic devices is driven by a large demand for faster and smaller systems. In the near future, colossal permittivity in nanomaterials will play a key role in the advances of electronic devices. We report on "colossal" permittivity values achieved in dense ceramics displaying ultrafine grain size ranging from 70 nm to 300 nm. Relative permittivity values of ~ $10^6$ at 1 kHz ($0.1 < \tan\delta < 0.7$) were obtained for $Ba_{0.95}La_{0.05}TiO_{3-x}$ ceramics. The colossal effective permittivity is related to an interfacial polarization and is achieved in nanomaterials by the activation of a high number of carriers and their trapping at the interfaces. Polarization carriers involving $Ti^{3+}$ polaron is proposed to be at the origin of the observed colossal permittivity. These results may have an important technological impact since these ceramics display ultrafine grain size opening a new route to the fabrication of very thin dielectric films.

High permittivity values such as $\varepsilon_r$ ~ 10 000 were reported in polycrystalline $BaTiO_3$, a well known ferroelectric material.[1] Decreasing the grain size below 0.7 μm of the $BaTiO_3$ ferroelectric ceramic was shown to yield unrelieved stresses resulting in smaller permittivity values.[2] Indeed, colossal permittivity values up to 200000 at room temperature were achieved in $BaTiO_3$ micronic grain size materials in which preparation included incorporation of metallic layers in a complex multi step process.[3,4] The achievement of high permittivity values in this material was ascribed to interfacial polarization phenomena. Recently, giant permittivity values were reported in hexagonal barium titanate (h-$BaTiO_3$) single crystals.[5,6] High permittivity values around $10^5$ measured on the oxygen deficient materials were explained by a Maxwell–Wagner interfacial polarization effect due to the presence of interfacial boundaries consisting of crystal defects such as screw dislocations. Nevertheless, the internal interfaces as well as the nature of the polarization carriers in the h-$BaTiO_3$ single crystals were not fully identified. Within the last few years, a large class of dielectric materials displaying colossal permittivity was proposed[7–9] with colossal dielectric constants mainly arising from extrinsic contributions of dielectric polarization such as Maxwell-Wagner interfacial polarization or internal barrier layer capacitor (IBLC) effect. For instance, colossal values of dielectric constant $3 \times 10^5$ reported for $Ca_{1.75}Pr_{0.25}MnO_4$ materials[8] were attributed to the Maxwell-Wagner polarization. Such colossal permittivity values have also been determined in $CaCu_3Ti_4O_{12}$ ceramics with grain size ~300 μm.[10] The large permittivity values of this material being attributed to the well established IBLC effect.[11] According to the brick layer model, the effective permittivity $\varepsilon_{eff}$ of the microstructure can be expressed as $\varepsilon_{eff} = \varepsilon_{gb}\ t_g/t_{gb}$ where $\varepsilon_{gb}$ is the grain boundary permittivity and $t_g$ and $t_{gb}$ are the thickness of the grain and grain boundary, respectively.[12] Thus the IBLC mechanism is usually associated with enhanced grain size. In this context, a decrease of the average grain size should not favor the IBLC effect and colossal permittivity in ultrafine ceramics, to our knowledge, has not been reported.

In this communication, we discuss the "colossal" permittivity values achieved in $BaTiO_{3-x}$ and $Ba_{0.95}La_{0.05}TiO_{3-x}$ materials exhibiting very small grain size (< 300 nm). Dense dielectrics ceramics were prepared from nanoscale chemically homogeneous powders by Spark Plasma Sintering[13] (SPS) method at two different temperatures (1323 and 1483 K). The sintered materials (above 97 % relative density) displayed a blue color due to the reducing sintering atmosphere.

$BaTiO_{3-x}$ nanomaterials, sintered at 1323 K are oxygen deficient, with residual carbon concentration as low as 100 ppm as revealed by FTIR measurements. Electron probe microanalysis (EPMA) showed a surprisingly large x value ($x = 0.37$). Since the tetragonal phase was reported as unstable for grain size lower than 0.7 μm,[2] our nanomaterial consists of an unexpected mixture of ~ 66 wt % of a tetragonal phase and ~ 33 wt % of cubic (or pseudo cubic) phase determined using the Rietveld method. This is consistent with previous results showing coexistence of both phases using the SPS technique with sub micrometer-sized grains.[14] Since our dense ceramics sintered by SPS methods are brittle, microstructure observations and identification of grain boundaries by microscopy investigation are difficult. However, an average grain size ~ 300 nm was determined (Fig. 1). A colossal

[*] Dr. J.-Y. Chane-Ching, Dr. S. Guillemet-Fritsch, Dr. Z. Valdez-Nava, Dr. C. Tenailleau, Prof. B. Durand
CIRIMAT, CNRS UMR 5085, Université Paul Sabatier
118, Route de Narbonne, 31062 Toulouse, Cedex 9 (France)
E-mail: chane@chimie.ups-tlse.fr
Dr. T. Lebey
LAPLACE, Université Paul Sabatier
118, Route de Narbonne, 31062 Toulouse, Cedex 9 (France)

[**] We thank G. Raimbeaux, C. Estournes for assistance on SPS sintering, performed at the PNF²-CNRS of Toulouse and C. Calmet for FEG-SEM micrographs. This work was supported by a Scientific Research Grant from the Ministry of Research of France.

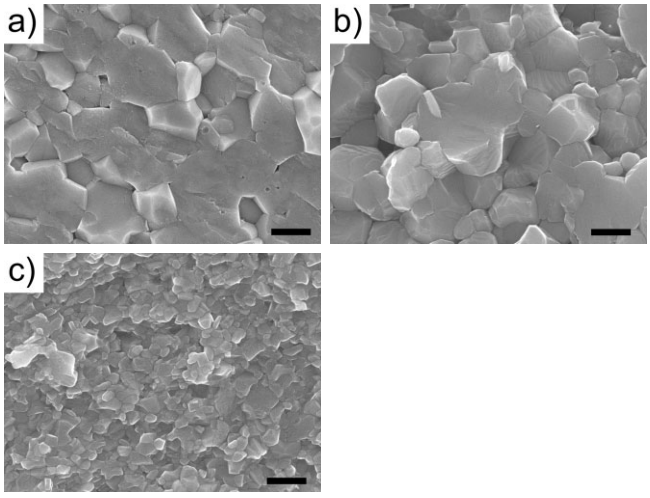


**Figure 1.** SEM micrographs of dense a) $BaTiO_{3-x}$ ceramics sintered at 1323 K with average grain size ~ 300 nm; b) $Ba_{0.95}La_{0.05}TiO_{3-x}$ prepared at 1483 K with average grain size ~300 nm and c) $Ba_{0.95}La_{0.05}TiO_{3-x}$ sintered at 1323 K with average grain size ~ 70 nm. Bar = 300 nm.

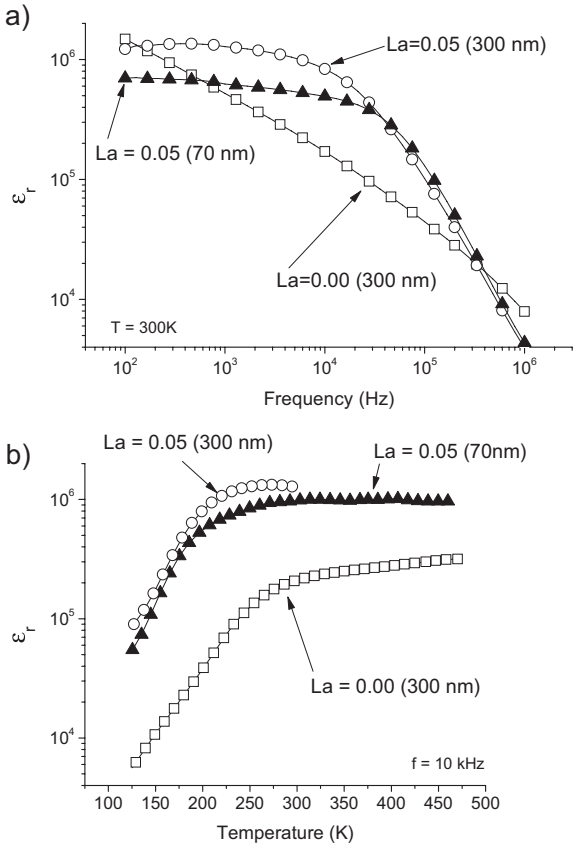


**Figure 2.** a) Frequency dependence at 300 K and b) temperature variation at 10 kHz of the real part of the dielectric response for nanosized $BaTiO_{3-x}$, (300 nm – 1323 K); $Ba_{0.95}La_{0.05}TiO_{3-x}$ (70 nm – 1323 K and 300 nm – 1483 K) dielectrics. A higher dispersion of the permittivity values is observed on the $BaTiO_{3-x}$ material compared to $Ba_{0.95}La_{0.05}TiO_{3-x}$. In b) for La = 0.05 (300 nm), data was not collected over 300 K due to high dielectric losses.

permittivity value ~ $0.8 \times 10^6$ was determined for this material at 300 K and 1 kHz with a dissipation factor, referred to as the loss tangent, tan$\delta$ = 0.56. A number of measurements with various electrodes displaying different work functions such as Au sputtered, or In screen printed electrodes showed that such colossal permittivity was not due to an electrode polarization effect. Figure 2 shows the frequency dependence of the permittivity at fixed temperatures. At 300 K, these plots show a colossal permittivity plateau occurring in a wide range of frequencies < 40 kHz. The temperature dependence of the permittivity at fixed frequencies highlights a gradual decrease of the colossal dielectric constant until about 300 K. Upon cooling below ~ 250 K, $\varepsilon_r$ drops dramatically by a factor of $10^5$. Such temperature dependence has already been observed in a number of materials and in particular in the h-$BaTiO_{3-x}$ single crystal,[6] with a characteristic temperature shift to 40 K. The lower characteristic temperature associated to the h-$BaTiO_3$ single crystal could be attributed either to a structural effect or a longer range structural order occurring in the single crystal. Obviously, this is in contrast with the results obtained for the polycrystalline nanomaterial in this study. Moreover, at this characteristic temperature, a higher dispersion of our permittivity values with temperature was observed compared to values previously reported for the single crystal h-$BaTiO_3$. This higher dispersion of permittivity values can also be observed with frequency. Since the nanomaterial is composed of a multitude of grains exhibiting various crystallizations, the observed dispersion may arise from a nanomaterial displaying a less homogeneous structure.

Impedance spectroscopy can be utilized in order to determine the main electrical characteristics of heterogeneous materials. Complex impedance spectra recorded on the broad 100–600 K temperature range can present two semi-circles modelled with an equivalent electrical circuit composed of two parallel (resistor R and capacitor C) elements connected in series. One RC element corresponds to the semi conducting grain which gives rise to a non zero intercept in the Z" vs Z' plots. The other RC element is attributed to grain boundary regions and the large arc intercept with the Z' gives a $R_{gb}$ value. In this study, the $R_{gb}$ value is ~ 14 MΩ·cm at room temperature. Decreasing the temperature in this study allowed a better separation of each contribution. We have been able to extract at a lower temperature of 140 K the R and C contributions from the grain as well as the grain boundaries. From the impedance spectroscopy analysis, the electrical properties of these ceramics ($R_{bulk}$ = 725 Ω·cm, $C_{bulk}$ < 55 nF cm$^{-1}$) and ($R_{gb}$ = 70 kΩ·cm, $C_{gb}$ = 650 nF cm$^{-1}$) have been found to be similar to those reported for the h-$BaTiO_3$ single crystal (see Table 1). Note that the low value of $R_{bulk}$ and the very low activation energy $E_a$ of ~ 0.07 eV determined for the grain boundaries of our ceramics differ from the values generally reported for polycrystalline $BaTiO_3$ materials.[15] However,

**Table 1.** Bulk and grain boundaries electrical characteristics, activation energies of $BaTiO_{3-x}$ (300 nm) and $Ba_{0.95}$ $La_{0.05}$ $TiO_{3-x}$ (300 and 70 nm) nanomaterials. $Ti^{3+}/Ti^{4+}$ ratios were determined by X-ray Photon Spectroscopy (XPS) on fresh fractured surfaces. R and C reported values were determined at 140 K for having better defined arc semi-circles at lower temperatures. Values corresponding to single crystal of h-$BaTiO_{3-x}$ are indicated for comparison.

| Material | $Ti^{3+}/Ti^{4+}$ ratio (th. density) | Bulk *R* [Ω·cm] $E_a$ [eV] | Bulk C [nF $cm^{-1}$] | Grain boundary *R* [Ω·cm] $E_a$ [eV] | Grain boundary *C* [nF $cm^{-1}$] |
|---|---|---|---|---|---|
| $BaTiO_{3-x}$ | 0.015 | 725 | <55 | 70000 | 650 |
| 300 nm | (~96%) | | | *$E_a$=0.07* | |
| *T* = 1323 K | | | | | |
| $Ba_{0.95}La_{0.05}TiO_{3-x}$ | 0.036 | 70 | 150 | 260 | 2200 |
| 300 nm | (~99%) | | | *$E_a$=0.07* | |
| *T* = 1483 K | | | | | |
| $Ba_{0.95}La_{0.05}TiO_{3-x}$ | 0.029 | 75 | 20 | 7500 | 2000 |
| 70 nm | (~96%) | | | *$E_a$=0.07* | |
| *T* =1323 K | | | | | |
| h-$BaTiO_3$ | | <20 | ~0.016 | >20000 | 6-10 |
| single | | (above 100 K) | (20-40 K) | (above 100 K) | (60-100 K) |
| crystal [5] | | $E_a$=0.03 | | *$E_a$=0.012* | |

this value must be compared to the 0.029 eV reported for the h-$BaTiO_3$ single crystal because our material exhibits well structured nanograins and quite well defined boundaries similar to the single crystal. This similarity could be ascribed to the flash sintering process involving specific conditions of reducing atmosphere, pressure, temperature and current.[13] Thus the large value of permittivity of the nanomaterial exhibiting a high structural homogeneity is due to a large number of carriers most likely involving polarization of almost all the population of grains.

Doping by $La^{3+}$ cation was previously reported to increase $BaTiO_3$ permittivity values.[15] To enable comparisons between non-doped and doped materials, we optimized the conditions of sintering ($T$ = 1483 K) for the doped material $Ba_{0.95}La_{0.05}TiO_{3-x}$ with $x$ ~ 0.38, to achieve the same comparable grain size of 300 nm. Similarly to the non-doped $BaTiO_{3-x}$ nanomaterial, a colossal dielectric constant ~ $1 \times 10^6$ at 1 kHz and room temperature was determined on the $Ba_{0.95}La_{0.05}TiO_{3-x}$ nanomaterial. However, the measured tanδ values become so large (tan$\delta$ >> 1) that the capacitive nature of the material is questionable. In comparison to the $BaTiO_3$ nanomaterial, complex impedance spectrum of the $Ba_{0.95}La_{0.05}TiO_{3-x}$ nanomaterial revealed a significant decrease in the bulk (70 Ω·cm) and grain boundary (260 Ω·cm) resistances that could correspond to either $La^{3+}$ doping or to the higher sintering temperature. These lower values can be attributed to a semi conducting bulk arising either from a charge balanced compensation mechanism occurring via the electronic ''La donor doping'' effect where $Ba^{2+} \rightarrow La^{3+} + e^-$ and subsequent formation of $Ti^{3+}$ or to the more reducing sintering atmosphere at higher temperature.[15] La doping in ultrafine grain size ceramics sintered at higher temperatures tends to improve the bulk conduction and diminishes the frequency and temperature dispersions of the permittivity as shown in Figure 2. From the resistances and tanδ determinations, there is also evidence for the creation of very low insulating grain boundaries that cannot act as effective barrier layers between semiconducting grains, which is unfavorable for possible industrial applications. However, improved insulation properties of the interfaces were achieved by decreasing the sintering temperature while maintaining a high level of bulk conduction. A $Ba_{0.95}La_{0.05}$-$TiO_{3-x}$ nanomaterial with $x$ ~ 0.36 and grain size as small as 70 nm was prepared by sintering at 1323 K, thus demonstrating the ability of the flash sintering process to produce ceramics without significant grain growth. The $Ba_{0.95}La_{0.05}TiO_{3-x}$ material sintered at 1323 K exhibits a permittivity of $0.8 \times 10^6$ at 300 K with dielectric loss, tan$\delta$ = 0.66 at 1 kHz. Lower values of tan $\delta$ ~ 0.1 were obtained on materials with permittivity values of ~ $0.3 \times 10^6$. The temperature and frequency profiles of the permittivity for $Ba_{0.95}La_{0.05}TiO_{3-x}$ materials sintered at 1323 and 1483 K are very close. Although no significant variation of the bulk resistance was observed, a decrease of the sintering temperature causes an increase of the grain boundary resistance from 260 Ω·cm to 7500 Ω·cm (see Table 1). The more insulating grain boundaries thus produce a larger charge carrier accumulation at the interfaces associated with a significant decrease of the losses of the nanomaterials as illustrated from the impedance plots showing a higher RC value for the low sintered temperature nanomaterials (Table 1 and Fig. 3).

The low frequency range of the phenomenon suggests an interfacial polarization mechanism.[16] Although no interfaces other than very small grain boundaries were detected up to now (interfaces width ~ 1 nm from high resolution transmission electron microscopy), it is possible that small internal boundaries and/or segregation of defects at the interfaces participate to the polarization mechanism.

With regards to the nature of the carriers, another important observation is the significant increase of the bulk conduction and barrier layer capacitance observed with $La^{3+}$ doping. Although $La^{3+}$ doping has been reported to diminish mass transport[17] yielding finer grain size in the sintered ceramic, we have here observed a drastic enhancement of bulk conduction by $La^{3+}$ doping. Indeed, $La^{3+}$ doping is associated with an increase in $Ti^{3+}$ concentration as revealed from X-ray Photon Spectroscopy (XPS) investigations on fresh fractured surfaces of ceramics. The importance of the presence of $Ti^{3+}$ was also reported in $CaCu_3Ti_4O_{12}$ dielectric material that exhibits a dielectric characteristic temperature of 150 K. In $CaCu_3Ti_4O_{12}$ dielectric materials, a polaron relaxation mecha-

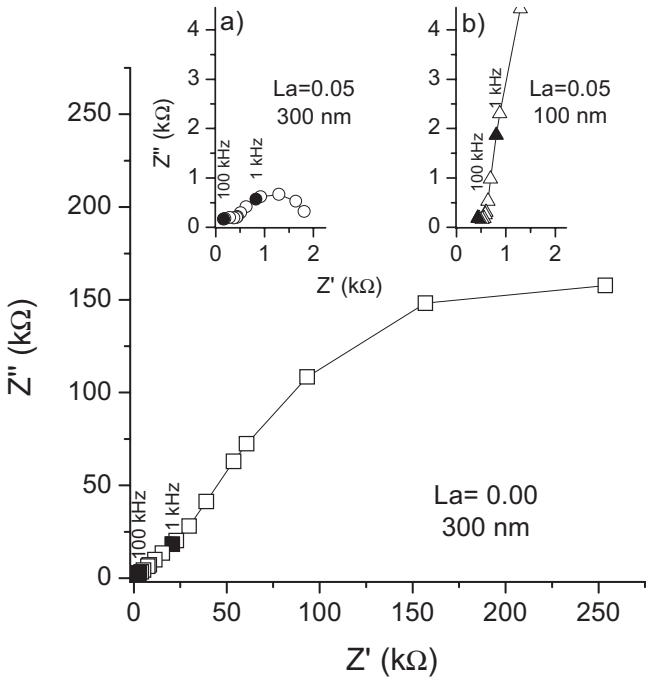


**Figure 3.** Impedance complex data for $BaTiO_{3-x}$ 300 nm. Insert, impedance plots for $Ba_{0.95}La_{0.05}TiO_{3-x}$ with grain size a) 300 nm and b) 70 nm. Note the higher values of R (axis of Z') for $BaTiO_{3-x}$ and the higher RC values displayed by the $Ba_{0.95}La_{0.05}TiO_{3-x}$ nanomaterial when sintered at lower temperature (1323 K). Data obtained at 140 K, with filled symbols indicating selected frequencies.

nism was reported and mixed valences of Ti ions were described to induce the high bulk polaron conduction of the dielectric grains.[18] In reduced $BaTiO_3$ materials, small polarons based on electronic hopping from successive Ti sites of $Ti^{3+}/Ti^{4+}$[19] associated with crystal defects such as oxygen vacancies ($V_o^{\circ\circ}$) have also been previously identified by Electronic Paramagnetic Resonance (EPR) signals.[20] Finally, we can state that the polarization phenomenon in our material is highly structurally dependent as previously shown. From all these observations, we suggest that these polarons act as possible carriers at the origin of the colossal permittivity. An intriguing feature related to the colossal permittivity nanomaterials is the low interface activation energy value, close to that value reported for the h-$BaTiO_3$ single crystal. This low activation energy value is consistent with the continuous O, Ti, and Ba concentration profiles that we have determined within single grain and across grain boundaries by Electron Energy Loss Spectroscopy (EELS). At this stage, the origin of the efficient blocking of the carriers at the insulating interfaces is still to be determined.

Achievement of colossal dielectric permittivity in nanomaterials requires the preparation of dense ceramics possessing highly semiconducting bulk grains that generate a high concentration of carriers in association with fine tuned grain boundaries displaying appropriate resistance. The insulating properties of the grain boundaries were shown to be promoted by sintering at low temperature. Therefore, at these low temperatures, nanosized powders are suitable to produce materials of high sintered density, a large $Ti^{3+}$ concentration and appropriate insulating grain boundaries. In addition, another interesting feature of the use of nanosized powders is the low correlation length of polarization arising from the ultrafine grains increasing thus the probability for each polarization carrier to reach the interface and contributing to the colossal dielectric polarization.

In conclusion, ultrafine ceramics displaying colossal dielectric permittivity were achieved in $BaTiO_{3-x}$ and $Ba_{0.95}La_{0.05}TiO_{3-x}$ materials, based on an interfacial polarization involving polarons due to the presence of $Ti^{3+}$ in all samples. In contrast to the complex multi-stage processing of dielectrics currently required to fabricate IBLCs, colossal dielectric permittivity nanomaterials displaying low bulk resistance with appropriate grain boundary resistance were produced in a single-step process. The use of ultrafine chemically homogeneous powders should lead to the fabrication of very thin dielectric films opening interesting routes for miniaturisation and development of integrated systems.[21]

## *Experimental*

$BaTiO_3$ and $Ba_{0.95}La_{0.05}TiO_3$ powders were synthesized by an oxalate precipitation route described elsewhere [22] using stoichiometric proportions of $BaCl_2 \cdot 2H_2O$, $LaCl_3 \cdot 7H_2O$ raw powders and $TiCl_3$ solution. Final products analyzed by field emission gun-scanning electron microscopy (FEG-SEM) showed 50 nm aggregated nanocrystals after calcination at 1123 K, with element contents in powders verified using inductively coupled plasma (ICP) emission spectroscopy. Dense dielectric ceramics of each composition were prepared from nanoscale and chemically homogeneous powders by Spark Plasma Sintering (SPS) method [13] at two different temperatures (1323 and 1483 K) for three minutes under 50 MPa and using a maximum current of 350 A, with rapid cooling. Gold or indium electrodes were used for electrical measurements. The frequency dependences of electrical characteristics were measured using an impedance analyser (HP LCR, model 4284A) in the $10^2$–$10^6$ Hz frequency range at room temperature. A dielectric analyzer (TA Instruments, model DEA 2940) was used over the 123–473 K temperature range and from $10^{-1}$–$10^5$ Hz in frequency.


[1] A. R. West, *Chem. Rec.* **2006**, *6*, 206.
[2] G. Arlt, D. Hennings, G. De With, *J. Appl. Phys.* **1985**, *58*, 1619.
[3] S. Jayanthi, T. R. N. Kutty, *J. Mater. Sci. Mater. Electron.* **2005**, *16*, 269.
[4] M. Valant, A. Dakskobler, M. Ambrozic, T. Kosmac, *J. Eur. Ceram. Soc.* **2006**, *26*, 891.
[5] J. Yu, P.-F. Paradis, T. Ishikawa, S. Yoda, *Appl. Phys. Lett.* **2004**, *85*, 2899.
[6] J. Yu, P.-F. Paradis, T. Ishikawa, S. Yoda, Y. Saita, M. Itoh, F. Kano, *Chem. Mater.* **2004**, *16*, 3973.
[7] N. Biskup, A. de Andres, J. L. Martinez, C. Perca, *Phys. Rev. B* **2005**, *72*, 024115.
[8] J. Mira, A. Castro-Couceiro, M. Sanchez-Andujar, B. Rivas-Murias, J. Rivas, M. A. Senaris-Rodriguez, *J. Phys. D* **2006**, *39*, 1192.

[9] C. C. Homes, T. Vogt, S. M. Shapiro, S. Wakimoto, A. P. Ramirez, *Science* **2001**, *293*, 673.
[10] T. B. Adams, D. C. Sinclair, A. R. West, *Phys. Rev. B* **2006**, *73*, 094124.
[11] D. C. Sinclair, T. B. Adams, F. D. Morrison, A. R. West, *Appl. Phys. Lett.* **2002**, *80*, 2153.
[12] R. Mauczok, R. Wernicke, *Philips Tech. Rev.* **1984**, *41*, 338.
[13] K. Inoue, *US Patent 3 250 892*, **1966**.
[14] M. T. Buscaglia, V. Buscaglia, M. Viviani, J. Petzelt, M. Savinov, L. Mitoseriu, A. Testino, P. Nanni, C. Harnagea, Z. Zhao, M. Nygren, *Nanotechnology* **2004**, *15*, 1113.
[15] F. D. Morrison, D. C. Sinclair, A. R. West, *J. Appl. Phys.* **1999**, *86*, 6355.
[16] A. J. Moulson, J. M. Herbert, *Electroceramics: Materials, Properties, Applications*, 2nd ed., Wiley, West Sussex, England **2003**.
[17] A. S. Janitzki, B. Hoffmann, P. Gerthsen, *J. Am. Ceram. Soc.* **1979**, *62*, 422.
[18] L. Zhang, Z.-J. Tang, *Phys. Rev. B* **2004**, *70*, 174306.
[19] O. Bidault, M. Maglione, M. Actis, M. Kchikech, B. Salce, *Phys. Rev. B* **1995**, *52*, 4191.
[20] S. Lenjer, O. F. Schirmer, H. Hesse, T. W. Kool, *Phys. Rev. B* **2002**, *66*, 165106.
[21] J. Junquera, P. Ghosez, *Nature* **2003**, *422*, 506.
[22] H. Yamamura, A. Watanabe, S. Shirasaki, Y. Moriyoshi, M. Tanada, *Ceram. Int.* **1985**, *11*, 17.